Symmetry reduction and semiclassical analysis of axially symmetric systems

Santanu Pal*
Variable Energy Cyclotron Centre, 1/AF Bidhan Nagar, Calcutta 700 064, India

Debabrata Biswas†
Center for Chaos and Turbulence Studies, Niels Bohr Institute, Blegdamsvej 17, Copenhagen Ø, Denmark

(Received 20 February 1996; revised manuscript received 24 September 1997)

We derive a semiclassical trace formula for a symmetry-reduced part of the spectrum in axially symmetric systems. The classical orbits that contribute are closed in (ρ,z,p_ρ,p_z) and have $p_\varphi=m\hbar$, where m is the azimuthal quantum number. For $m\neq 0$, these orbits vary with energy and almost never lie on periodic trajectories in the full phase space in contrast to the case of discrete symmetries. The transition from $m=0$ to $m>0$, however, is not as dramatic as our numerical results indicate, suggesting that contributing orbits occur in topologically equivalent families within which p_φ varies smoothly. [S1063-651X(98)02401-5]

PACS number(s): 05.45.+b, 03.65.Sq

I. INTRODUCTION

Modern semiclassical theories deal with the duality of the quantum energy eigenspectrum and the classical spectrum of periodic orbit lengths and stabilities [1]. For integrable systems, the Poisson summation formula provides this connection and is equivalent to the Einstein-Brillouin-Keller quantization scheme, while for generic quantum systems, trace formulas deal with this duality and provide the only connection between quantum and classical mechanics. As an example, for hyperbolic systems the Gutzwiller trace formula expresses the density of quantum energy eigenvalues $d(E)=\sum_n \delta(E-E_n)$ as

$$d(E)=d_{av}(E)+\frac{1}{\pi\hbar}\sum_p \sum_{r=1}^{\infty} \frac{T_p}{\sqrt{|\det(M_p^r-I)|}} \times\cos(rS_p-\pi\sigma_p r/2), \tag{1.1}$$

where the summation over p extends over all primitive periodic orbits, T_p is the corresponding time period, S_p is the action, σ_p is the Maslov index associated with its invariant manifolds [2], and M_p is the stability matrix arising from a linearization of the transverse flow. For systems where periodic orbits occur in families, appropriate modifications need to be made [3,4], though these may be system specific [5].

Quite often, the systems we encounter in nuclear, atomic, or molecular physics have symmetries and one might be interested in the spectrum of a particular symmetry class. For example, billiard systems with reflection symmetry about the x and y axes have four classes of wave functions with a choice of Dirichlet or von Neumann boundary condition on the symmetry lines. In these as well as in other systems with discrete symmetries, it is possible to construct the symmetry-reduced Green's function and evaluate its trace [6]. While the orbits that contribute are periodic in the reduced phase space, they are not necessarily periodic in the full phase space. The end points, however, are related by symmetry. It nevertheless turns out that when allowed to evolve in time, these orbits are eventually periodic in the full phase space. Thus trajectories contributing to any given symmetry class of the spectrum are either full periodic orbits or parts of these whenever the symmetries present are discrete in nature [6,7].

The presence of continuous symmetries implies the existence of constants of motion. For example, in systems with axial symmetry, the z component of the angular momentum is conserved and quantum mechanically one may be interested in the spectrum of a particular m subspace. A way to deal with this problem semiclassically is to work with an effective two-dimensional potential $V(\rho,z)+\hbar^2m^2/2M\rho^2$, where M is the mass of the particle and m is the azimuthal quantum number. Here $V(\rho,z)$ is the actual potential in which the dynamics is executed and the additional term $\hbar^2m^2/2M\rho^2$ arises from the conservation of l_z [8,9]. The semiclassical trace formula then takes the form in Eq. (1.1) provided periodic orbits are isolated and unstable.

An alternative procedure is to work with the dynamics in the full phase space and it is desirable to understand the nature of the trace formula and the kind of classical orbits that contribute. We shall devote ourselves to this question throughout the rest of this paper and our results are, in a certain sense, very different from those for discrete symmetry. The orbits that contribute necessarily have an angular momentum $l_z=m\hbar$ and must close in ρ,p_ρ and z,p_z. Thus they are not necessarily periodic since they need not close in φ. Unlike discrete symmetries, however, orbits that are not periodic are generally not parts of periodic orbits. We support these results with extensive numerical evidence.

On completion of this work, we came across a paper by Creagh [10] that deals with this problem for arbitrary Abelian symmetries and rotational symmetry. Our approaches are different however. Creagh [10] takes recourse to group-theoretical methods in order to obtain the symmetry-reduced Green's function and then uses a semiclassical approximation that ultimately involves classical trajectories possessing quantized values of these additional constants of motion. Our approach is based on the fact that for axially symmetric systems, the eigenfunction $\psi(\rho,\varphi,z)=(2\pi)^{-1/2}e^{im\varphi}\phi(\rho,z)$ and

*Electronic address: santanu@veccal.ernet.in
†Permanent address: Theoretical Physics Division, Bhabha Atomic Research Center, Bombay 400 085, India. Electronic address: biswas@kaos.nbi.dk

we use this in the full Green's function to obtain the density of a given m subspace. The restriction of constants of motion to their quantized values arises from a stationary phase condition in our case as well as the fact that the trajectory must close in ρ, p_ρ and z, p_z. Thus, even though the final results are identical, the derivation in this paper provides an alternate viewpoint that is simple and transparent to those not familiar with the intricacies of extended phase space.

Apart from a rederivation of the trace formula and its numerical verification, this work emphasizes the fact that orbits contributing to a symmetry-reduced part of the spectrum in general are not eventually periodic in the full phase space whenever the symmetry is continuous. This is an important departure from the case of discrete symmetry. We also show that contributing orbits occur in topologically equivalent families within which p_φ varies smoothly. For successive m therefore, distinct orbits from the same family contribute and this is evident from the shift of peaks in the power spectrum of the quantum density.

The organization of the paper is as follows. In Sec. II we provide a derivation of the trace formula. Section III deals with the inverse problem that motivates our numerical results which we present in Sec. IV. Our conclusions are summarized in Sec. V.

II. FORMALISM

Let us consider an axially symmetric three-dimensional system described by the coordinates (φ, η), where φ is the azimuthal angle about the axis of symmetry and $\eta = (\eta_2, \eta_3)$ represents the other two components in an orthogonal coordinate system. The basic definition of the full Green's function of such a system can be written as

$$G(\varphi'' \eta'', \varphi' \eta'; E) = \sum_n \sum_m \frac{\psi_n^{(m)}(\varphi'' \eta'') \psi_n^{(m)\dagger}(\varphi' \eta')}{E - E_{n,m}}, \tag{2.1}$$

where

$$\psi_n^{(m)}(\varphi, \eta) = \frac{\exp(im\varphi)}{\sqrt{2\pi}} \phi_n^{(m)}(\eta). \tag{2.2}$$

In the above, both ψ and ϕ are taken to be normalized and m is the azimuthal quantum number. Thus

$$G(\varphi'' \eta'', \varphi' \eta'; E) = \frac{1}{2\pi} \sum_m \exp[im(\varphi'' - \varphi')] \times \sum_n \frac{\phi_n^{(m)}(\eta'') \phi_n^{(m)\dagger}(\eta')}{E - E_{n,m}}. \tag{2.3}$$

Multiplying both sides by $\exp(-i\mu\varphi'')$ and integrating over φ'', one obtains

$$\sum_n \frac{\phi_n^{(\mu)}(\eta'') \phi_n^{(\mu)\dagger}(\eta')}{E - E_{n,\mu}} = \int_0^{2\pi} G(\varphi'' \eta'', \varphi' \eta'; E) \times \exp[-i\mu(\varphi'' - \varphi')] d\varphi'' \tag{2.4}$$

where $\{E_{n,\mu}\}$ is the subset of eigenvalues for which the azimuthal quantum number equals μ. Further integration over φ' on both sides gives

$$\sum_n \frac{\phi_n^{(\mu)}(\eta'') \phi_n^{(\mu)\dagger}(\eta')}{E - E_{n,\mu}} = \frac{1}{2\pi} \int_0^{2\pi} \int_0^{2\pi} G(\varphi'' \eta'', \varphi' \eta'; E) \times \exp[-i\mu(\varphi'' - \varphi')] d\varphi'' d\varphi'. \tag{2.5}$$

Equation (2.5) can be viewed as the symmetry-reduced Green's function corresponding to the azimuthal quantum number μ. A semiclassical expression for this can be obtained by using the semiclassical approximation to the full Green's function

$$G(\varphi'' \eta'', \varphi' \eta'; E) \simeq \frac{2\pi}{(2\pi i\hbar)^2} \sum_{\text{cl tr}} \sqrt{|\det[D(\varphi'' \eta'', \varphi' \eta'; E)]|} \times \exp\left[\frac{i}{\hbar} S(E) - \frac{i}{2} \nu\pi\right], \tag{2.6}$$

which has contributions from all classical trajectories (cl tr) at energy E connecting points (φ'', η'') and (φ', η'). The action $S(E)$ is

$$S(\eta'', \eta', \varphi, E) = \int_{\varphi' \eta'}^{\varphi'' \eta''} p \, dq = \int_{\eta'}^{\eta''} p_\eta d\eta + p_\varphi(\varphi'' - \varphi' + 2\pi N) = \overline{S}(\eta'', \eta', p_\varphi, E) + p_\varphi(\varphi + 2\pi N), \tag{2.7}$$

where p_φ is a constant of motion due to the axial symmetry of the system, $\varphi = \varphi'' - \varphi'$, N is the winding number, and $\overline{S}$ is the reduced action $\int_{\eta'}^{\eta''} p_\eta d\eta$. Final, ν is the Maslov index, which is determined by the caustics encountered along the trajectory [2], while the matrix D is given by [1]

$$D(\varphi'' \eta'', \varphi' \eta'; E) = \frac{\partial(p_{\varphi''}, p_{\eta''}, t)}{\partial(\varphi', \eta', E)} = \begin{pmatrix} \frac{\partial^2 S}{\partial\varphi' \partial\varphi''} & \frac{\partial^2 S}{\partial\varphi' \partial\eta''} & \frac{\partial^2 S}{\partial\varphi' \partial E} \\ \frac{\partial^2 S}{\partial\eta' \partial\varphi''} & \frac{\partial^2 S}{\partial\eta' \partial\eta''} & \frac{\partial^2 S}{\partial\eta' \partial E} \\ \frac{\partial^2 S}{\partial E \partial\varphi''} & \frac{\partial^2 S}{\partial E \partial\eta''} & \frac{\partial^2 S}{\partial E^2} \end{pmatrix}. \tag{2.8}$$

In order to arrive at a semiclassical form for the symmetry-reduced Green's function, we insert Eq. (2.6) into Eq. (2.5) and use a new set of variables $\varphi=\varphi''-\varphi'$ and $\overline{\varphi}=(\varphi''+\varphi')/2$ to obtain

$$\sum_n \frac{\phi_n^{(\mu)}(\eta'')\phi_n^{(\mu)\dagger}(\eta')}{E-E_{n,\mu}} \simeq \frac{1}{(2\pi i\hbar)^2}\sum_{\text{cl tr}} \int_0^{2\pi} d\overline{\varphi}\int_{-\pi}^{\pi} d\varphi \times\exp[-i\mu\varphi]\sqrt{|\det(D)|} \times\exp\left[\frac{iS}{\hbar}-\frac{i\nu\pi}{2}\right], \tag{2.9}$$

where we have used

$$\int_0^{2\pi}\int_0^{2\pi} d\varphi' d\varphi'' = \int_{-\pi}^{\pi} d\varphi \int_0^{2\pi} d\overline{\varphi}. \tag{2.10}$$

We shall evaluate the integral over φ using the method of stationary phase in the limit $\hbar\to 0$. The stationarity condition

$$\frac{\partial S}{\partial\varphi}-\mu\hbar=0 \tag{2.11}$$

restricts trajectories to quantized values of p_φ $(=\partial S/\partial\varphi)$. We shall denote the stationary point by φ^* such that $p_\varphi(\varphi^*)=\mu\hbar$. The integration yields

$$\sum_n \frac{\phi_n^{(\mu)}(\eta'')\phi_n^{(\mu)\dagger}(\eta')}{E-E_{n,\mu}} \simeq \frac{1}{(2\pi i\hbar)^{3/2}}\sum_{\text{cl tr}} \int_0^{2\pi} d\overline{\varphi}\frac{\sqrt{|\det[D(\varphi^*,\eta'',\eta';E)]|}}{\sqrt{|U|}} \times\exp\left[\frac{i\overline{S}}{\hbar}-\frac{i\nu'\pi}{2}\right], \tag{2.12}$$

where $U=\partial^2 S/\partial\varphi^2=\partial p_\varphi/\partial\varphi$ evaluated at the stationary point φ^* and $\nu'=\nu+\beta'$ with $\beta'=1$ if U is negative and zero otherwise. We shall postpone the $\overline{\varphi}$ integration, but for now we merely note that the symmetry of the system allows this to be evaluated exactly.

The semiclassical symmetry-reduced Green's function is thus expressed as a sum of contributions from classical trajectories at an energy E, connecting points η'' and η' and having an angular momentum $p_\varphi=\mu\hbar$. We can now simplify the ratio of the amplitude determinants and express $|\det(D)|/|U|$ as

$$\frac{|\det(D)|}{|U|}=\frac{|\det(D)|}{\left|\dfrac{\partial^2 S}{\partial\varphi'\partial\varphi''}\right|}=|\det(\widetilde{D})|, \tag{2.13}$$

where

$$\widetilde{D}=\begin{pmatrix} \dfrac{\partial^2\overline{S}}{\partial\eta'\partial\eta''} & \dfrac{\partial^2\overline{S}}{\partial\eta'\partial E} \\ \dfrac{\partial^2\overline{S}}{\partial E\partial\eta''} & \dfrac{\partial^2\overline{S}}{\partial E^2}\end{pmatrix}. \tag{2.14}$$

Details of this reduction can be found in the Appendix.

It is useful at this point to introduce a local coordinate system (η_2,η_3) in the reduced (η) plane, where η_2 changes along the trajectory while η_3 increases in the transverse direction and is zero on the orbit. It follows from the definition that

$$\frac{\partial^2\overline{S}}{\partial E\partial\eta_2''}=\frac{1}{\dot\eta_2''},\quad \frac{\partial^2\overline{S}}{\partial\eta_2'\partial E}=-\frac{1}{\dot\eta_2'} \tag{2.15}$$

and

$$\frac{\partial^2\overline{S}}{\partial\eta_i'\partial\eta_2''}=0=\frac{\partial^2\overline{S}}{\partial\eta_2'\partial\eta_i''}, \tag{2.16}$$

so that the determinant ratio can be expressed as

$$\det(\widetilde{D})=\left\{\frac{1}{\dot\eta_2''}\frac{1}{\dot\eta_2'}\left(-\frac{\partial^2\overline{S}}{\partial\eta_3'\partial\eta_3''}\right)\right\}_{\varphi=\varphi^*}=\frac{1}{\dot\eta_2''}\frac{1}{\dot\eta_2'}R. \tag{2.17}$$

With these simplifications, we are now ready to evaluate the trace of the symmetry-reduced Green's function. Setting $\eta''=\eta'=\eta$ and integrating over η on both sides of Eq. (2.12), we get

$$g_\mu(E)=\sum_n \frac{1}{E-E_{n,\mu}}\simeq\frac{1}{(2\pi i\hbar)^{3/2}}\sum_{\text{cl tr}}\int_0^{2\pi} d\overline{\varphi}\oint d\eta\frac{1}{\dot\eta_2}\sqrt{|R|} \times\exp\left[\frac{i\overline{S}}{\hbar}-\frac{i\nu'\pi}{2}\right], \tag{2.18}$$

where g_μ is the trace of the symmetry-reduced Green's function corresponding to the azimuthal quantum number μ, $\overline{S}=\oint p_\eta d\eta$, and

$$R=\left\{-\frac{\partial^2\overline{S}}{\partial\eta_3'\partial\eta_3''}\right\}_{\varphi=\varphi^*,\,\eta'=\eta''}. \tag{2.19}$$

Clearly, the only orbits that contribute to the trace are the ones that have $p_\varphi=\mu\hbar$ and are closed in η but not necessarily in φ. Further, the η integration can be performed by the method of stationary phase and the stationarity condition then picks only that subset of orbits for which $p_{\eta'}=p_{\eta''}$ at $\eta'=\eta''=\eta$. We shall refer to such trajectories in the full three-dimensional (3D) dynamics as quasiperiodic trajectories (QPTs) since they will be periodic in the reduced dynamics of the η motion. In what follows such periodic orbits in the reduced system will be referred to as reduced periodic orbits (RPOs).

The action $\overline{S}$ in the neighborhood of a RPO can thus be written to second order as $\overline{S}(\eta_3,E)=\overline{S}(\eta_3=0;E)+(\eta_3^2/2)W$, where

$$W=\left[\frac{\partial^2\overline{S}}{\partial\eta_3''\partial\eta_3''}+2\frac{\partial^2\overline{S}}{\partial\eta_3''\partial\eta_3'}+\frac{\partial^2\overline{S}}{\partial\eta_3'\partial\eta_3'}\right]_{\eta_3''=\eta_3'=0}. \tag{2.20}$$

On performing the η_3 integration by the method of stationary phase, Eq. (2.18) reduces to

$$g_\mu(E)\simeq\frac{1}{2\pi i\hbar}\sum_{\rm QPT}\int_0^{2\pi}d\overline{\varphi}\oint\frac{d\eta_2}{\dot{\eta}_2}\sqrt{\left|\frac{R}{W}\right|}_{\eta_3=0}\times\exp\left[\frac{i}{\hbar}\overline{S}(E)-i\frac{\pi}{2}\sigma\right], \tag{2.21}$$

where $\sigma=\nu'+\beta$ with $\beta=1$ if W is negative and zero otherwise. As in the case without symmetry, σ is the Maslov index of the stable or unstable manifold and is an invariant of the reduced periodic orbit [2].

While we do not explicitly show this, the factor involving the second derivatives of $\overline{S}$ is related to linearized dynamics in the neighborhood of the RPO and is expressed as [1]

$$\sqrt{\left|\frac{\left(\frac{\partial^2\overline{S}}{\partial\eta_3'\partial\eta_3''}\right)_{\eta_3''=\eta_3'=0}}{\left(\frac{\partial^2\overline{S}}{\partial\eta_3''\partial\eta_3''}+2\frac{\partial^2\overline{S}}{\partial\eta_3''\partial\eta_3'}+\frac{\partial^2\overline{S}}{\partial\eta_3'\partial\eta_3'}\right)_{\eta_3''=\eta_3'=0}}\right|}=\frac{1}{\sqrt{|\det(M-I)|}}, \tag{2.22}$$

where the 2×2 matrix M is the stability matrix describing the dynamics in the linearized neighborhood of the RPO and I is the unit matrix. Note that σ is independent of the position η_2 along the periodic orbit and so are $\overline{S}(E)$ and $\sqrt{|\det(M-I)|}$. The integration along η_2 thus yields

$$\oint\frac{d\eta_2}{\dot{\eta}_2}=T_0, \tag{2.23}$$

where T_0 is the period of the primitive RPO or, in terms of the time $T_{\rm QPT}$ required to span the QPT in the full 3D dynamics, $T_0=T_{\rm QPT}/N_0$, where N_0 is the number of primitive RPOs contained in the quasiperiodic trajectory. It is instructive, however, to deal with the $\eta_2,\overline{\varphi}$ integrations together and this yields the ''volume'' of initial conditions for which the various stationarity conditions are satisfied. Thus,

$$\int_0^{2\pi}d\overline{\varphi}\oint\frac{d\eta_2}{\dot{\eta}_2}=W_0, \tag{2.24}$$

where $W_0=\overline{\Phi T}=2\pi T_0=2\pi T_{QPT}/N_0$. Note that when the QPT is also periodic and has an N_1 fold symmetry, one can interpret $\overline{\Phi}=2\pi/N_1$ and $T=T_{\rm QPT}/r=T_p$ when viewed in the full phase space. Here r is the repetition number of the periodic orbit in the full phase space and $rN_1=N_0$. With these clarifications, Eq. (2.21) becomes

$$g_\mu(E)\simeq\frac{1}{2\pi i\hbar}\sum_{\rm QPT}\frac{2\pi T_0}{\sqrt{|\det(M-I)|}}\exp\left[\frac{i}{\hbar}\overline{S}(E)-\frac{i}{2}\sigma\pi\right]. \tag{2.25}$$

This is the main result of this section. The sum involves quasiperiodic trajectories at an energy E and with $p_\varphi=\mu\hbar$ and is identical to the result obtained by Creagh [10].

It is instructive, however, to examine the significance of Eq. (2.11) in greater detail. In performing the φ integration for each orbit, it is implicit that the action changes smoothly as the orbit (characterized by φ and hence p_φ) is varied. In other words, orbits occur in topologically equivalent families [11] within which the action varies smoothly and the stationary phase condition of Eq. (2.11) picks out one orbit from this family. By changing μ, another orbit from the same family contributes and this has a slightly different value of $\overline{S}$. The range of μ over which a family contributes depends on its extent, which in turn is decided by the potential $V(\rho,z)$. These ideas are put on a more concrete footing for axially symmetric cavities in the following sections.

It is easy to check that the trace of the full Green's function is recovered by summing over μ as

$$\sum_\mu g_\mu(E)=\sum_N\int d\mu\, g_\mu(E)\exp(2\pi i\mu N) \tag{2.26}$$

$$\simeq\frac{1}{i\hbar}\frac{1}{2\pi}\sum_N\int d\mu\sum_{\rm QPT}\frac{2\pi T_0}{\sqrt{|\det(M-I)|}}\times e^{(i/\hbar)\{\overline{S}+2\pi\mu\hbar N\}-i\sigma\pi/2}, \tag{2.27}$$

where we have used the Poisson summation formula and substituted Eq. (2.25) for $g_\mu(E)$. The integral, when evaluated by the method of stationary phase, picks up only those trajectories for that $\partial\overline{S}/\partial p_\varphi+2\pi N=0$ or $\varphi^*=2\pi N$. Thus the only orbits that contribute to the full spectrum are the ones that are periodic in the full phase space. The final expression is

$$g(E)\simeq\frac{1}{i\hbar(2\pi i\hbar)^{1/2}}\sum_{\rm PO}\frac{(2\pi/N_1)T_p}{\sqrt{|\det(M-I)|}}\sqrt{\left|\frac{\partial p_\varphi}{\partial\varphi}\right|}\times\exp\left[\frac{i}{\hbar}S_p(E)-\frac{i}{2}\sigma_p'\pi\right], \tag{2.28}$$

with $\sigma'=\sigma-\delta$, where $\delta=1$ or 0 depending on whether $\partial^2\overline{S}/\partial p_\varphi^2$ is positive or negative. The result is identical to that obtained by Creagh and Littlejohn [3,12].

For the sake of completeness, it is necessary to mention that there is yet another contribution to the trace that we have so far neglected. It arises from the *zero-length orbits* and gives rise to the average density of states $d_{\rm av}^\mu(E)$ and to the leading order this is given by [13,10]

$$d^{\mu}_{\rm av}(E)=\frac{1}{h^3}\int dp\ dq\ \hbar\ \delta(p_{\varphi}-\mu\hbar)\,\delta(E-H(p,q)). \tag{2.29}$$

Equation (2.25) gives the oscillatory part of the density $d^{\mu}_{\rm osc}(E)=-(1/\pi)\lim_{\epsilon\to 0^+}{\rm Im}g_{\mu}(E+i\epsilon)$, where Im denotes the imaginary part. In the following sections we shall illustrate our results for axially symmetric cavities and look at contributions of QPTs in $d^{\mu}_{\rm osc}(E)$ as well as the μ dependence of $d^{\mu}_{\rm av}(E)$.

Though we have restricted ourselves to the case of axial symmetry, the formalism is very general and can be adapted to other cases of continuous symmetry. For example, in the case of rotational symmetry, one can express the wave function as

$$\psi^{(l,m)}_n(r,\theta,\varphi)=Y^m_l(\theta,\varphi)\,\phi^{(m,l)}_n(r)\,, \tag{2.30}$$

where $\{Y^m_l(\theta,\varphi)\}$ are the spherical harmonics. This can be used in Eq. (2.1) to obtain the trace of the Green's function for a given value of the quantum numbers l and m.

III. AXIALLY SYMMETRIC CAVITY

We now specialize to the case of a particle moving freely inside an axially symmetric cavity and undergoing specular reflections on a collision with the wall. As in most other systems, it is easier to verify the duality in Eq. (2.25) starting with quantum levels and obtaining the length spectrum of periodic orbits. This is easily achieved by computing the power spectrum of the quantum density $d^{\mu}(\sqrt{E})$:

$$S^{\mu}(l)=\left|\int dk\ d^{\mu}(k)\exp\{ikl\}\right| \tag{3.1}$$

$$=\left|\int dk(d^{\mu}_{\rm av}+d^{\mu}_{\rm osc})\exp\{ikl\}\right|, \tag{3.2}$$

where $\sqrt{E}=k$ and $d^{\mu}(k)=2kd_{\mu}(k^2)$ is the quantum density for a given value of μ. The average part of the quantum density gives rise to a peak at zero in $S^{\mu}(l)$, while the oscillatory part contributes peaks at the length of quasiperiodic orbits with $p_{\varphi}=\mu\hbar$.

What is perhaps not apparent is the fact that for $\mu\neq 0$, the reduced periodic orbits that contribute to $d^{\mu}_{\rm osc}$ vary with energy whenever they are not periodic (i.e., $\varphi\neq 0$). These peaks are therefore expected to shift in the power spectrum with the window over which it is computed.

Consider, for example, an orbit in the equatorial plane ($z=0$) where the particle reflects specularly inside a circular billiard of radius R. It is easy to see that two successive points on the caustic [14] (one reflection between them) satisfy the conditions for quasiperiodicity since $\rho'=\rho''$, $z'=z''=0$, $p'_{\rho}=p''_{\rho}$, and $p'_z=p''_z=0$. The action on this QPT is thus $S_j=\sqrt{E}l_j$, where $l_j=2R\sin(\varphi/2)$, where φ is the difference in angle $\varphi''-\varphi$ between these points on the caustic. By moving away from the caustic to a point along the trajectory, there exists another point separated by a collision where conditions for quasiperiodicity are satisfied (i.e., $\rho'=\rho''$ and $p'_{\rho}=p''_{\rho}$). It is also easy to check that along this quasiperiodic orbit, φ is conserved while φ changes by moving from the caustic in the radial direction to another orbit of the same topological family. The stationary phase condition in Eq. (2.11) is thus

$$p_{\varphi}=\sqrt{E}R\cos(\varphi/2)=\mu\hbar \tag{3.3}$$

or, equivalently

$$\varphi^{*}=2\cos^{-1}(\mu\hbar/R\sqrt{E}), \tag{3.4}$$

so that

$$\overline{S_j}=2R\sqrt{E}\sqrt{1-\frac{\mu^2\hbar^2}{R^2E}}-2\mu\hbar\cos^{-1}(\mu\hbar/R\sqrt{E}) \tag{3.5}$$

in Eq. (2.25). For $\mu\neq 0$, the orbit varies with energy continuously and the system is thus inhomogeneous. At a given (nonzero) value of μ, the length of the contributing orbit increases with energy and thus should give rise to broadened peaks in the power spectrum $S^{\mu}(l)$.

Note that the stationarity condition in Eq. (3.3) picks up one orbit for each μ from this topologically equivalent family of one-bounce orbits within which p_{φ} varies smoothly. In spite of the complicated dependence of $\overline{S}$ on E and μ, it is evident that with increasing μ, peaks in the power spectrum $S^{\mu}(l)$ shift to the left. Moreover, the broadening of peaks is expected to increase with μ due to a larger spread in the length of contributing orbits.

An interesting consequence of this analysis is the fact that at almost all energies this quasiperiodic trajectory is not eventually periodic in the full phase space whenever $\mu\neq 0$. This follows from the fact that periodic orbits in the circle billiard form a set of measure zero. This conclusion also holds in the more general case. For $\mu\neq 0$, whenever a reduced periodic orbit corresponds to a periodic orbit in the full phase space with $p_{\varphi}=\mu\hbar$, the action $\overline{S_j}=\sqrt{E}l_j-2\pi N_j\mu\hbar$, where N_j is the winding number of the orbit. However, on changing the energy E this orbit no longer has the quantized value of p_{φ} and hence cannot contribute. Similar arguments hold for QPTs that form part of periodic orbits in the full phase space. Thus, at any energy, most orbits that contribute to $d^{\mu}_{\rm osc}$ do not lie on a trajectory that is periodic in the full phase space. This phenomenon is in sharp contrast to the case of discrete symmetries where all quasiperiodic trajectories are eventually periodic in the full phase space. The only exception is the trivial case $\mu=0$ when all reduced periodic orbits lie on periodic trajectories in the full phase space. Though we have restricted ourselves to a simple orbit in the preceding analysis, the conclusions are in fact more general as the numerical results of the following section indicate.

We now return to an evaluation of the average density of states $d^{\mu}_{\rm av}(E)$ for cavities where Eq. (2.29) becomes

$$d^{\mu}_{\rm av}(E)=\frac{1}{h^3}\int dp_{\rho}dp_z dp_{\varphi}dz\ d\rho\ d\varphi\ \hbar\ \delta(p_{\varphi}-\mu\hbar)$$

$$\times\delta\left(E-p^2_{\rho}-p^2_z-\frac{p^2_{\varphi}}{\rho^2}\right) \tag{3.6}$$

for a particle of mass $M=1/2$. The integrals are straightforward to evaluate and the final result is expressed as

$$d_{\rm av}^{\mu}(E)=\frac{1}{4\pi\hbar^2}A', \tag{3.7}$$

where

$$A'=\int_{z_{\rm min}^{\mu}}^{z_{\rm max}^{\mu}}dz\int_{\rho_{\rm min}^{\mu}}^{\rho_{\rm max}}d\rho. \tag{3.8}$$

Note that $z_{\rm min}^{\mu}, z_{\rm max}^{\mu}, \rho_{\rm min}^{\mu}$ depend on μ and are dictated by the centrifugal barrier, while $\rho_{\rm max}$ depends on z through the shape of the cavity. For small $|\mu|/\sqrt{E}$, however, $A'\simeq A-Z_0R_0$, where Z_0 is the extent of the cavity along the Z axis and $R_0=|\mu|\hbar/\sqrt{E}$. Thus

$$d_{\rm av}^{\mu}(E)\simeq\frac{A}{4\pi}\frac{1}{\hbar^2}-\frac{|\mu|Z_0}{4\pi}\frac{1}{\sqrt{E}}\frac{1}{\hbar}, \tag{3.9}$$

where

$$A=\int_{z_{\rm min}^{0}}^{z_{\rm max}^{0}}dz\int_{0}^{\rho_{\rm max}}d\rho \tag{3.10}$$

is the area of the ρZ plane. Consequently, the average integrated density of states $N_{\rm av}^{\mu}(E)=\int_0^E d_{\rm av}^{\mu}(E')dE'$ is

$$N_{\rm av}^{\mu}(E)=\frac{AE}{4\pi}-\frac{|\mu|Z_0}{2\pi}\sqrt{E}, \tag{3.11}$$

where for convenience we have set $\hbar=1$.

Note that the first term in the expression for $N_{\rm av}^{\mu}(E)$ is identical to that for a two-dimensional billiard of area A. We have not evaluated the standard perimeter term here, which is of the same order as the second term of Eq. (3.11), though as we shall show later, Eq. (3.11) predicts the correct μ dependence for cavities.

IV. SOME NUMERICAL RESULTS

We present here some numerical results on an axially symmetric cavity described by

$$R(\theta)=\frac{R_0}{\lambda}\{1+\alpha_n P_n(\cos\theta)\}, \tag{4.1}$$

where R_0 is the radius of a sphere having the same volume as the deformed cavity, λ is a volume preserving factor, α_n is the strength of the deformation, and $\{P_n\}$ are the Legendre polynomials. $R(\theta)$ is the distance from the origin to a point on the surface of the cavity, which due to the axial symmetry depends only on the angle θ measured from the Z axis. For our calculations, we choose a $P_2\,(n=2)$ deformed cavity with $R_0=1$, $\lambda=1.008\,087$, and $\alpha_2=0.2$. For convenience, we choose the mass $M=1/2$ and $\hbar=1$. Details of the procedure used in obtaining the quantum energy eigenvalues can be found in [15].

We have made no attempt towards finding periodic orbits systematically for this system because there is no obvious symbolic dynamics that one can use and also since we are interested in the inverse problem. While orbits in the XY plane are well known, we have determined periodic orbits in the YZ plane ($p_\varphi=0$) using the orbit length extremization technique. We believe that the list we have compiled is complete for lengths $l<15$. Figure 1 shows a plot of two periodic orbits that also satisfy the condition $p_{\eta'}=p_{\eta''}$ at points separated by half their total lengths.

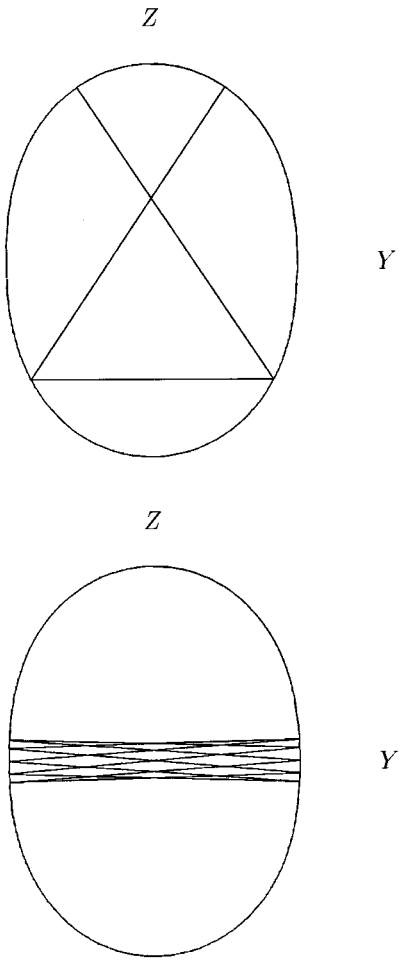

FIG. 1. Two periodic orbits in the YZ plane on which points separated by half the total length satisfy the conditions $z'=z'',\rho'=\rho''$ and $p_{z'}=p_{z''},p_{\rho'}=p_{\rho''}$. Their respective lengths are 11.532 715 and 17.856 224 in units of R_o.

In Figs. 2–4 we show plots of the power spectrum $S^{\mu}(l)$ for $\mu=(0,1),(2,4),(6,8)$. The small arrows mark the position of full periodic orbits in the YZ plane and the orbit along the diameter in the XY plane, while the larger arrows mark those orbits that do not close in φ. All of these have $p_\varphi=0$ and hence orbits that do not enclose φ form part of the periodic orbits. The peaks in the power spectrum for $\mu=0$ agree very well with the lengths of quasiperiodic orbits marked by arrows, though there is no distinct peak at 4.7615 or 9.5230. These correspond to the periodic orbit along the Z axis and its repetition. Unlike other orbits that occur in a one-parameter family, this orbit is isolated and hence has a much smaller contribution. We shall return to this later while discussing states belonging to a particular parity class.

The $\mu=1$ power spectrum is also described well by these orbits that have $p_\varphi=0$. The peaks shift to the left only slightly, indicating that the topology of the orbit does not

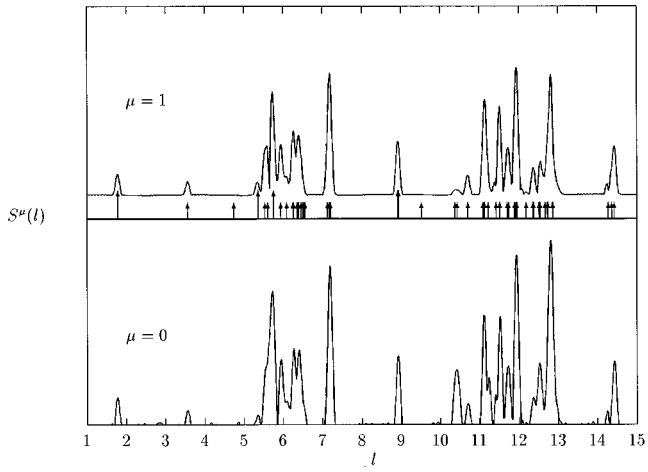

FIG. 2. Power spectrum $S^{\mu}(l)$ (in arbitrary units) of $\mu=0$ and 1 states. The shorter set of arrows marks the lengths (in units of R_o) of full periodic orbits in the YZ plane, while the longer arrows are quasiperiodic trajectories in the YZ plane that do not close in φ. All trajectories have $p_{\varphi}=0$.

change while going from $p_{\varphi}=0$ to a nonzero value of p_{φ}. The phenomenon can be understood from the analysis in Sec. III, where we have explicitly described the orbit selection process for the simplest orbit in the XY plane. The only significant change occurs at 10.38, where the peak height decreases appreciably.

This process continues for larger values of μ and can be seen from the power spectrum. The peaks gradually shift to the left of the arrow and nothing dramatic happens except that at $\mu=4$, there is no trace of the orbit at $l=10.38$. There is yet another feature that is readily seen by comparing the power spectra of $\mu=0$ or 1 and $\mu=8$. The peaks broaden significantly with increasing μ even though there is hardly any change in the range of eigenvalues considered for evaluating the power spectrum. This is due to the fact that the length of the orbit (belonging to a topologically equivalent family) varies with energy and its spread around the mean value increases with the value of μ.

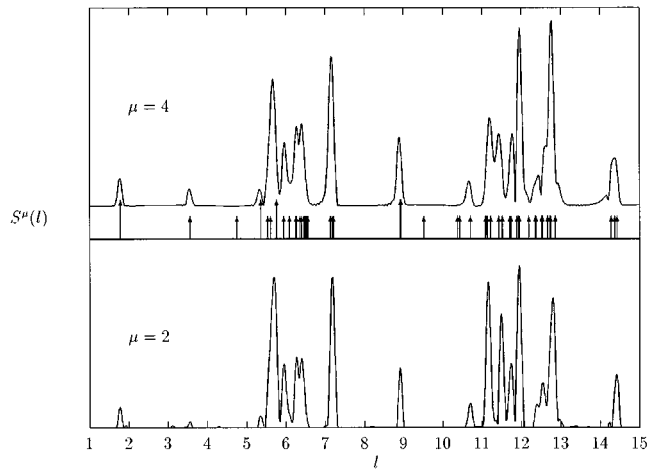

FIG. 3. Power spectrum $S^{\mu}(l)$ (in arbitrary units) of $\mu=2$ and 4 states. The arrows mark the length (in units of R_o) of orbits with $p_{\varphi}=0$ as in Fig. 2.

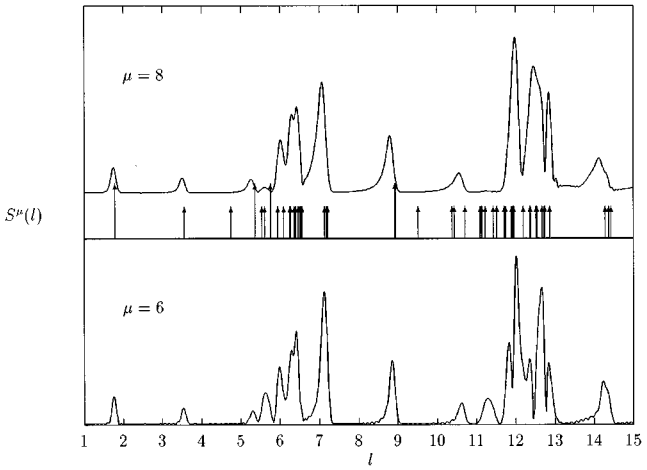

FIG. 4. Power spectrum $S^{\mu}(l)$ (in arbitrary units) of $\mu=6$ and 8 states. The arrows mark the length (in units of R_o) of orbits with $p_{\varphi}=0$ as in Fig. 2.

We emphasize this aspect in Fig. 5 where we plot the power spectrum for $\mu=26$ for two different windows of energy. The one centered at the higher energy has peaks significantly to the right of the other, indicating that the lengths of contributing orbits increase with energy. We also compare the power spectrum of $\mu=1$ and $\mu=26$ in Fig. 6 and find that for the simplest (topological) orbit family (connecting successive points on the caustic) the peaks for $\mu=26$ are broader and to the left of the corresponding peak for $\mu=1$.

These findings corroborate our results of the previous sections and we now investigate the power spectrum of even or odd parity states for a particular value of μ. Contributions to the semiclassical symmetry reduced even or odd Green's function come from two sources. Apart from the usual orbits with $p_{\varphi}=\mu\hbar$ connecting (ρ',z',φ') and (ρ'',z'',φ'') there are additional contributions from orbits having $p_{\varphi}=\mu\hbar$ connecting points (ρ',z',φ') and $(\rho'',-z'',\varphi''+\pi)$ weighted appropriately by the character of the symmetry group [6]. Alternately, one can exploit the additional φ symmetry and express the symmetry-reduced even or odd (denoted respectively as $+$ or $-$) Green's function as

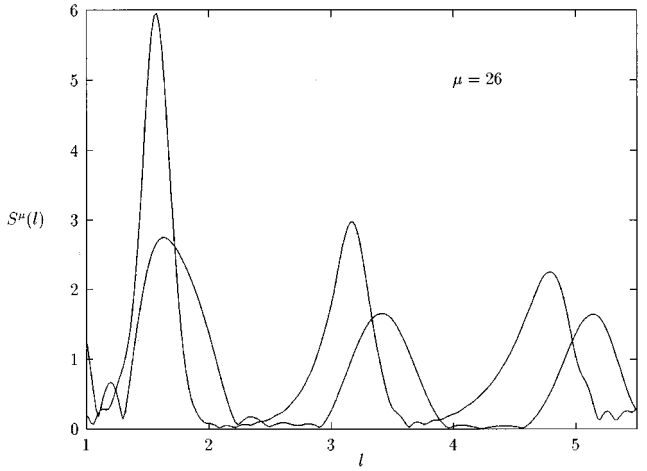

FIG. 5. Power spectrum (in arbitrary units) of $\mu=26$ states for two different ranges of energy. The window centered at higher energy has peaks shifted to the right. The lengths are in units of R_o.

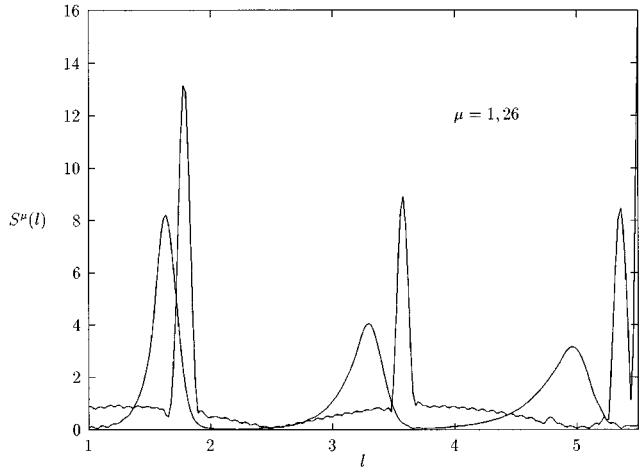

FIG. 6. Comparison of the power spectrum (in arbitrary units) of $\mu=1$ and 26 states. The $\mu=26$ spectrum gives rise to broader peaks due to a larger spread in the lengths of contributing orbits. The window is approximately over the same range of energy in both cases. The lengths are in units of R_o.

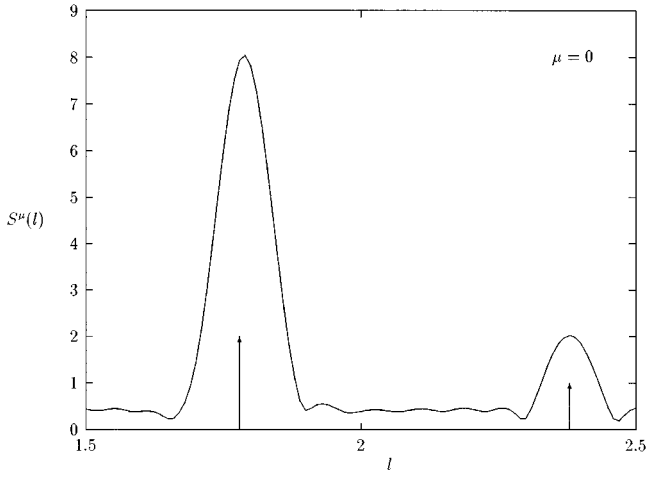

FIG. 7. Power spectrum (in arbitrary units) of $\mu=0$, even-parity states. The smaller arrow marks the length (in units of R_o) of the half orbit along the Z axis.

$$\sum_{n_1} \frac{\phi^{(\mu)}_{n_1}(\rho,z)\phi^{(\mu)\dagger}_{n_1}(\rho,z)}{E-E^{\pm}_{n_1,\mu}}$$
$$= \frac{1}{4\pi}\Bigg[\int_0^{2\pi}\int_0^{2\pi} G(\varphi'',\rho,z;\varphi',\rho,z;E)\exp[-i\mu(\varphi''-\varphi')]d\varphi''d\varphi' \pm (-1)^{\mu}\int_0^{2\pi}\int_0^{2\pi} G(\varphi'',\rho,-z;\varphi',\rho,z;E)\exp[-i\mu(\varphi''-\varphi')]d\varphi''d\varphi'\Bigg]. \quad (4.2)$$

The trace of its semiclassical version thus involves quasiperiodic trajectories with $p_{\varphi}=\mu\hbar$ *and* trajectories connecting (ρ,z) with $(\rho,-z)$ having $p_{\varphi}=\mu\hbar$ and $p_z^f=-p_z^i$, where f and i refer respectively to the initial and final points.

Thus we expect to see both full and half QPTs in the power spectrum of even parity and odd parity sequences. In particular, the half orbit along the Z axis will have a lower damping (due to its instability, the damping is exponential with the length of the orbit) and hence could be visible in the power spectrum. This is indeed obvious in Fig. 7, where a peak appears at $l=2.38$. In fact, a closer observation also reveals a peak at $l=4.76$. Significantly, orbits belonging to the XY plane do not have any other symmetry-related orbit and hence have no additional peak at half the length.

Finally, we study the μ dependence of the average density by plotting $k_N^{(\mu)}-k_N^{(0)}$ as a function of the level number N in Fig. 8. Here $k_N^{\mu}=\sqrt{E_N^{\mu}}$. An approximate expression for $k_N^{(\mu)}-k_N^{(0)}$ can be obtained using Eq. (3.11) and is given by

$$k_N^{(\mu)}-k_N^{(0)} \simeq \frac{|\mu|Z_0}{A}+\sqrt{\frac{\mu^2 Z_0^2}{A^2}+\frac{4\pi N}{A}}-\sqrt{\frac{4\pi N}{A}}. \quad (4.3)$$

Therefore, for large N, $k_N^{(\mu)}-k_N^{(0)}\simeq|\mu|Z_0/A$ and for the cavity that we have considered, this is $1.38|\mu|$.

Figure 8 is a plot of $k_N^{(\mu)}-k_N^{(0)}$ for $\mu=1$ (bottom curve) to $\mu=6$ (top curve). Each curve is approximately constant and the mean separation between curves is $1.38|\mu|$, as predicted.

V. CONCLUSIONS

In the previous sections we have studied the semiclassics of symmetry-reduced spectra for the case of axial symmetry. There are two approaches to the problem. The first exploits the conservation of l_z to reduce the system to two dimensions. Orbits then move around in an effective potential that includes the centrifugal term $\hbar^2m^2/2M\rho^2$. In comparison, the approach that we adopt here uses the dynamics in the full phase space and the trace formula then takes a different structure altogether. Our aim has been to understand the nature of the classical trajectories that contribute and also point out the differences with the case of discrete symmetry.

Most of this paper deals with a derivation of the trace formula for the spectrum with a given value μ of the azimuthal quantum number m. Though this has been studied by Creagh [10] earlier, we provide an independent derivation here using only the structure of the wave function to achieve

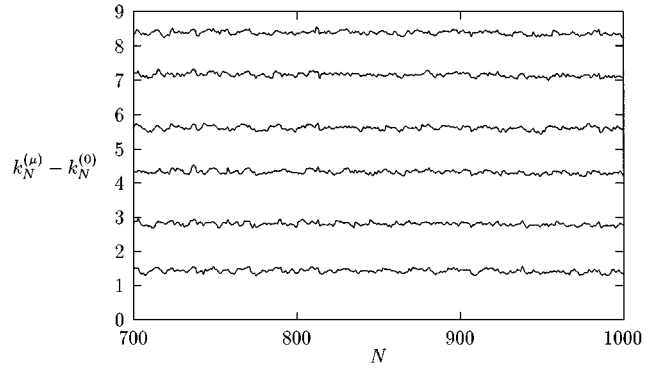

FIG. 8. Plot of $k_N^{(\mu)}-k_N^{(0)}$ (in units of R_o^{-1}) as a function of the level number N. The curves from bottom to top are (in order of increasing μ) for $\mu=1$ to $\mu=6$.

symmetry reduction. Finally, though we have worked with axially symmetric systems, the method can in principle be extended to a large class of systems with continuous symmetry.

Our main results are the following.

(i) The average density $d^{\mu}_{\rm av}(E)=A/4\pi-(|\mu|Z_0/4\pi)(1/\sqrt{E})$ for small $|\mu|/\sqrt{E}$ so that $k_N^{(\mu)}-k_N^{(0)}\simeq Z_0/A$, where N denotes the level number and $k_N=\sqrt{E_N}$.

(ii) The only classical trajectories that contribute to the oscillatory part of the quantum spectrum $d^{\mu}_{\rm osc}(E)$ are those that are closed in (ρ,z,p_ρ,p_z) and for which $p_\varphi=\mu\hbar$. Thus they need not be closed in the full phase space, though they may be eventually periodic when allowed to evolve. These orbits are, however, periodic in the reduced phase space (ρ,z,p_ρ,p_z).

(iii) For $\mu=0$, all reduced periodic orbits are identical to or part of periodic orbits in the full phase space.

(iv) For $\mu\neq 0$, almost all orbits that contribute to $d^{\mu}(E)$ at any given energy are nonperiodic in the full phase space even when they are allowed to evolve in time. Peaks in the power spectrum thus shift with the window over which it is computed and the width of peaks increases with μ.

Our numerical results support these observations and allow us to state the following: For smooth potentials (billiards with smooth boundaries), topologically equivalent orbits contribute at successive values of μ as can be seen from the gradual shift in the position of peaks in the power spectrum. This is implicit in the selection criterion in Eq. (2.11) since each of the orbits selected necessarily occurs in a (topological) family within which p_φ varies smoothly. The transition from $\mu=0$ to $\mu\neq 0$ is therefore smooth and this might have some significance in quantizing the spectrum for $\mu=1$ using information about contributing orbits at $\mu=0$.

ACKNOWLEDGMENTS

D.B. acknowledges several useful and interesting discussions with Bertrand Georgeot and Gregor Tanner and thanks Stephen Creagh for several clarifications.

APPENDIX

We outline here the steps involved in the reduction of the amplitude determinants leading to Eq. (2.13). The equation for the reduced action

$$\overline{S}(\eta'',\eta',p_\varphi,E)=S(\eta'',\eta',\varphi,E)-p_\varphi\varphi \tag{A1}$$

is a Legendre transformation from the variables (η'',η',φ,E) to the variables $(\eta'',\eta',p_\varphi,E)$ and leads to the relations

$$\frac{\partial S}{\partial\eta_i'}=\frac{\partial\overline{S}}{\partial\eta_i'},\quad \frac{\partial S}{\partial\eta_i''}=\frac{\partial\overline{S}}{\partial\eta_i''},\quad \frac{\partial S}{\partial E}=\frac{\partial\overline{S}}{\partial E},$$

$$\frac{\partial S}{\partial\varphi}=p_\varphi,\quad \frac{\partial\overline{S}}{\partial p_\varphi}=-\varphi. \tag{A2}$$

The following expressions involving the second derivatives of the action can now be derived:

$$\frac{\partial^2 S}{\partial\eta_i'\partial\eta_j''}=\frac{\partial^2\overline{S}}{\partial\eta_i'\partial\eta_j''}+\frac{\partial^2\overline{S}}{\partial p_\varphi\partial\eta_i'}\frac{\partial^2\overline{S}}{\partial p_\varphi\partial\eta_j''}\frac{\partial^2 S}{\partial\varphi^2}, \tag{A3a}$$

$$\frac{\partial^2 S}{\partial\eta_i'\partial E}=\frac{\partial^2\overline{S}}{\partial\eta_i'\partial E}+\frac{\partial^2\overline{S}}{\partial p_\varphi\partial\eta_i'}\frac{\partial^2\overline{S}}{\partial p_\varphi\partial E}\frac{\partial^2 S}{\partial\varphi^2}, \tag{A3b}$$

$$\frac{\partial^2 S}{\partial\eta_i''\partial E}=\frac{\partial^2\overline{S}}{\partial\eta_i''\partial E}+\frac{\partial^2\overline{S}}{\partial p_\varphi\partial\eta_i''}\frac{\partial^2\overline{S}}{\partial p_\varphi\partial E}\frac{\partial^2 S}{\partial\varphi^2}, \tag{A3c}$$

$$\frac{\partial^2 S}{\partial E^2}=\frac{\partial^2\overline{S}}{\partial E^2}+\frac{\partial^2\overline{S}}{\partial p_\varphi\partial E}\frac{\partial^2\overline{S}}{\partial p_\varphi\partial E}\frac{\partial^2 S}{\partial\varphi^2}, \tag{A3d}$$

$$\frac{\partial^2 S}{\partial\varphi^2}=-\left(\frac{\partial^2\overline{S}}{\partial p_\varphi^2}\right)^{-1}, \tag{A3e}$$

$$\frac{\partial^2 S}{\partial\eta_i'\partial\varphi}=\frac{\partial^2\overline{S}}{\partial p_\varphi\partial\eta_i'}\frac{\partial^2 S}{\partial\varphi^2}, \tag{A3f}$$

$$\frac{\partial^2 S}{\partial\eta_i''\partial\varphi}=\frac{\partial^2\overline{S}}{\partial p_\varphi\partial\eta_i''}\frac{\partial^2 S}{\partial\varphi^2}, \tag{A3g}$$

$$\frac{\partial^2 S}{\partial\varphi\partial E}=\frac{\partial^2\overline{S}}{\partial p_\varphi\partial E}\frac{\partial^2 S}{\partial\varphi^2}. \tag{A3h}$$

We shall derive Eq. (A3a) as an illustration:

$$\frac{\partial^2 S}{\partial\eta_i'\partial\eta_j''}=\frac{\partial}{\partial\eta_i'}\left(\frac{\partial S}{\partial\eta_j''}\right)=\frac{\partial}{\partial\eta_i'}\left(\frac{\partial\overline{S}}{\partial\eta_j''}(\eta'',\eta',p_\varphi,E)\right)$$
$$=\frac{\partial^2\overline{S}}{\partial\eta_i'\partial\eta_j''}+\frac{\partial^2\overline{S}}{\partial p_\varphi\partial\eta_j''}\frac{\partial p_\varphi}{\partial\eta_i'}.$$

Also,

$$\frac{\partial^2\overline{S}}{\partial p_\varphi\partial\eta_i'}=\frac{\partial}{\partial p_\varphi}\left(\frac{\partial S}{\partial\eta_i'}(\eta'',\eta',\varphi,E)\right)=\frac{\partial^2 S}{\partial\varphi\partial\eta_i'}\frac{\partial\varphi}{\partial p_\varphi},$$

so that

$$\frac{\partial p_\varphi}{\partial\eta_i'}=\frac{\partial^2\overline{S}}{\partial p_\varphi\partial\eta_i'}\frac{\partial^2 S}{\partial\varphi^2}. \tag{A4}$$

Thus

$$\frac{\partial^2 S}{\partial \eta_i' \partial \eta_j''} = \frac{\partial^2 \overline{S}}{\partial \eta_i' \partial \eta_j''} + \frac{\partial^2 \overline{S}}{\partial p_\varphi \partial \eta_j''} \frac{\partial^2 \overline{S}}{\partial p_\varphi \partial \eta_i'} \frac{\partial^2 S}{\partial \varphi^2}. \quad \text{(A5)}$$

We are now in a position to deal with the ratio of determinants. By interchanging rows and columns, the determinant of Eq. (2.8) can be expressed as

$$\det(D) = \det \begin{pmatrix} \frac{\partial^2 S}{\partial \eta' \partial \eta''} & \frac{\partial^2 S}{\partial \eta' \partial E} & \frac{\partial^2 S}{\partial \eta' \partial \varphi''} \\ \frac{\partial^2 S}{\partial E \partial \eta''} & \frac{\partial^2 S}{\partial E^2} & \frac{\partial^2 S}{\partial E \partial \varphi''} \\ \frac{\partial^2 S}{\partial \varphi' \partial \eta''} & \frac{\partial^2 S}{\partial \varphi' \partial E} & \frac{\partial^2 S}{\partial \varphi' \partial \varphi''} \end{pmatrix}$$

$$= \frac{\partial^2 S}{\partial \varphi' \partial \varphi''} \det(\overline{D} - \overline{E}), \quad \text{(A6)}$$

where

$$\overline{D} = \begin{pmatrix} \frac{\partial^2 S}{\partial \eta' \partial \eta''} & \frac{\partial^2 S}{\partial \eta' \partial E} \\ \frac{\partial^2 S}{\partial E \partial \eta'} & \frac{\partial^2 S}{\partial E^2} \end{pmatrix} \quad \text{(A7)}$$

and

$$\overline{E} = \begin{pmatrix} \frac{\partial^2 S}{\partial \eta' \partial \varphi''} \\ \frac{\partial^2 S}{\partial E \partial \varphi''} \end{pmatrix} \left(\frac{\partial^2 S}{\partial \varphi' \partial \varphi''} \right)^{-1} \begin{pmatrix} \frac{\partial^2 S}{\partial \varphi' \partial \eta''} & \frac{\partial^2 S}{\partial \varphi' \partial E} \end{pmatrix}$$

$$= \left(\frac{\partial^2 S}{\partial \varphi' \partial \varphi''} \right)^{-1} \begin{pmatrix} \frac{\partial^2 S}{\partial \eta' \partial \varphi''} \frac{\partial^2 S}{\partial \varphi' \partial \eta''} & \frac{\partial^2 S}{\partial \eta' \partial \varphi''} \frac{\partial^2 S}{\partial \varphi' \partial E} \\ \frac{\partial^2 S}{\partial E \partial \varphi''} \frac{\partial^2 S}{\partial \varphi' \partial \eta''} & \frac{\partial^2 S}{\partial E \partial \varphi''} \frac{\partial^2 S}{\partial \varphi' \partial E} \end{pmatrix}.$$

Using relations (A3a)–(A3h), it follows that

$$\det(\widetilde{D}) = \det D \left(\frac{\partial^2 S}{\partial \varphi' \partial \varphi''} \right)^{-1} = \det(\overline{D} - \overline{E})$$

$$= \det \begin{pmatrix} \frac{\partial^2 \overline{S}}{\partial \eta' \partial \eta''} & \frac{\partial^2 \overline{S}}{\partial \eta' \partial E} \\ \frac{\partial^2 \overline{S}}{\partial E \partial \eta''} & \frac{\partial^2 \overline{S}}{\partial E^2} \end{pmatrix}. \quad \text{(A8)}$$

[1] M.C. Gutzwiller, *Chaos in Classical and Quantum Mechanics* (Springer, New York, 1990); in *Chaos and Quantum Physics*, 1989 Lectures, Les Houches, edited by M.-J. Giannoni, A. Voros, and J. Zinn-Justin (North-Holland, Amsterdam, 1991).

[2] J.M. Robbins, Nonlinearity **4**, 343 (1991); S. Creagh, J.M. Robbins, and R.G. Littlejohn, Phys. Rev. A **42**, 1907 (1990).

[3] S. Creagh and R. Littlejohn, Phys. Rev. A **44**, 836 (1991).

[4] S. Creagh and R. Littlejohn, J. Phys. A **25**, 1643 (1992).

[5] P.J. Richens and M.V. Berry, Physica D **2**, 495 (1981).

[6] J.M. Robbins, Phys. Rev. A **40**, 2128 (1989).

[7] P. Cvitanović and B. Eckhardt, Nonlinearity **6**, 277 (1993).

[8] (ρ, φ, z) are cylindrical coordinates. In the corresponding Cartesian coordinate system, the axis of symmetry is the Z axis and the $z = 0$ plane is the XY plane.

[9] H. Friedrich and D. Wintgen, Phys. Rep. **183**, 37 (1989).

[10] S. Creagh, J. Phys. A **26**, 95 (1993).

[11] The phrase *topologically equivalent family* is used in a sense that is distinct from the usual *one-parameter family* in which all orbits exist due to the axial symmetry and within which the action is constant.

[12] See also p. 65 of S. Creagh, Ann. Phys. (N.Y.) **248**, 60 (1996). The apparent difference between the phase appearing therein and the present phase σ' arises due to different ways of defining the azimuthal angle, but nevertheless they lead to the same value for both the phases.

[13] B. Lauritzen and N. Whelan, Ann. Phys. (N.Y.) **244**, 112 (1995).

[14] For a circle, this is the point of nearest approach from the center.

[15] T. Mukhopadhay and S. Pal, Nucl. Phys. A **592**, 291 (1995).